Supporting information for

Experimental and theoretical investigation on facet-dependent MoO_2/BiOBr Z-scheme heterojunction photocatalytic nitrogen reduction: modulation of bulk charge separation efficiency by built-in electric field intensity

Zhuying Chen[a], Zhiling Huang[b], Jieyi Yang[a], Yue Meng[b], Bo Xie[a], Zheming Ni[a], Shengjie Xia[a,*]

[a] *Department of Chemistry, College of Chemical Engineering, Zhejiang University of Technology, Hangzhou 310014, P. R. China*

[b] *Department of Pharmaceutical Engineering, School of Life and Health Sciences, Huzhou College, Huzhou 313000, P. R. China*

* Corresponding author.

E–mail: xiasj@zjut.edu.cn (S.J. Xia)

Telephone number: 086–0571–88320373

1. Characterization

X−ray diffraction (XRD) patterns were recorded with a PANalytical Empyrean powder diffractometer using Cu Kα radiation (λ= 0.1541 nm). The working voltage was 45 kV and the working current was 40 mA. The patterns were collected with a 2θ range from 10° to 80° at a step of 0.0167°. The UV−2600 UV−spectrophotometer was used to analyze the optical absorption properties and the forbidden band width of the material with $BaSO_4$ as the background, a slit width of 2.0 nm, a scanning speed of 1.0 nm/s, and a scanning range of 200−800 nm. A scanning electron microscope (Gemini 500, Zeiss company, Germany) to analyze the morphology of the prepared samples. The structure and elemental distribution were studied with a Tecnai G2 F30 transmission electron microscope (TEM) (accelerating voltage of 300 kV). The chemical composition and valence of the materials were analyzed by Thermo Scientific K−Alpha X−ray photoelectron spectroscopy (XPS) instrument. The light source used for electrochemical testing is a 300 W xenon lamp with a 20 s interval (20 s on, 20 s off). The surface photovoltage test equipment consists of a lock-in amplifier (SR830) light chopper with monochromatic light provided by a 500 W xenon lamp through a monochromatic grating instrument. The German Bruker EMXplus-6/1 paramagnetic resonance spectrometer was used to test the hydroxyl and superoxide radicals of the catalyst. Perform the above tests on the electrochemical workstation CHI750E by dispersing 10 mg of the powder sample in 1 mL of ultrapure water/ethanol solution, and then adding 50 μL Nafion solution, sonicate for 30 minutes to form a uniform suspension. Drip 100 μL suspension onto ITO glass, air dry at room temperature for photoelectric testing. The testing conditions for transient photocurrent and electrochemical impedance are: illumination time interval of 20 seconds (20 seconds on and 20 seconds off), with more than 4 cycles; Light source: 300 W xenon lamp; Bottom solution: 0.5 M Na_2SO_4 solution. The Mott Schottky test frequency is 2000 Hz, and the substrate is a 0.5 M Na_2SO_4 solution.

2. Photocatalytic ammonia synthesis experiment

The photocatalytic ammonia synthesis experiments were carried out at room temperature, and the experimental setup is shown in **Figure S1**. The specific

experimental process is as follows: 10 mg of catalyst was dispersed in 40 mL of ultrapure water and sonicated for 10 min. Subsequently, stirring (400 rpm/min) was turned on to ensure homogeneous dispersion of the system. Afterwards, N_2 (99.999%) was introduced and the flow rate of N_2 was controlled to be 80−100 mL/min. The system was bubbled for 30 min in the dark and protected from light to remove the air. Afterwards, a 300 W Xe lamp (PL−X300D, light intensity of 22.06 W/cm^2) was turned on for the photocatalytic ammonia synthesis experiment. Every 20 min, 2 mL of reaction solution was collected and added to the detection solution, and NH_4^+ was detected by salicylic acid method, and the amount of ammonia production was calculated by the standard curve (**Figure S2**).

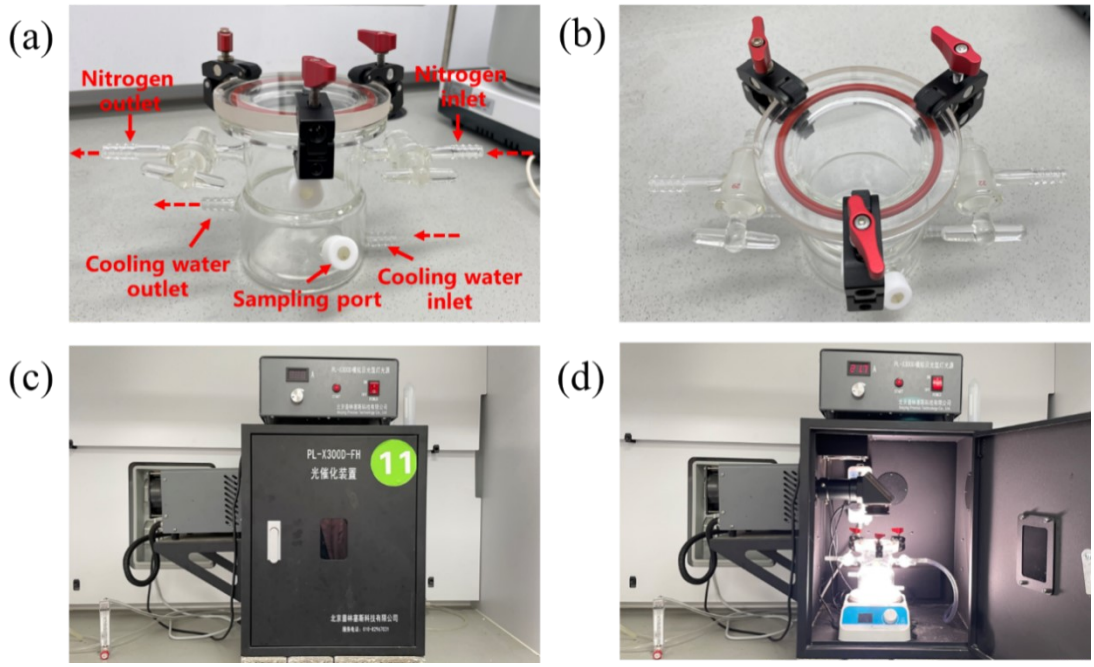

Figure S1. Schematic diagram of Photocatalytic ammonia setup: photocatalytic quartz reactor (a, side view; b, top view) and Xe light sources (c and d).

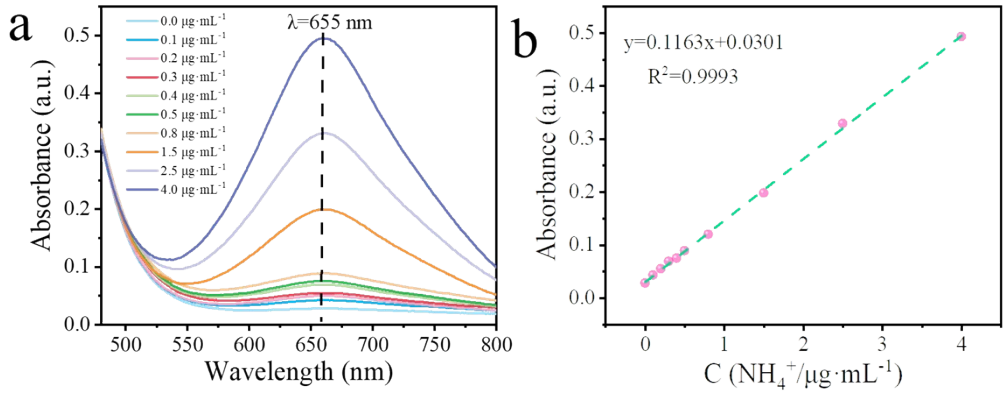

Figure S2. (a) The UV−visible absorption spectrum of NH_4^+; (b) Standard curve of Salicylic acid method for detecting NH_4^+ (C is the concentration, A is the absorbance).

3. Density functional theory calculations

All first-principles spin polarization calculations were performed by using the Cambridge Sequential Total Energy Package (CASTEP) module of the Materials Studio 8.0 software. The generalized gradient approximation (GGA) in the Perdew−Burke–Ernzerhof (PBE) form and a cutoff energy of 489.8 eV for planewave basis set were adopted, and the projector augented−wave (PAW) potential was used to represent the core-valence electron interaction. The MoO_2 (110) crystal plane was constructed from optimized MoO_2 cells with lattice parameters of a = 5.620 Å, b = 4.644 Å, c = 5.628 Å, α = γ= 90°, β= 109.87°, optimized in calculations using a 1 × 2 × 1 k−point grid, while electronic structure calculations were performed using a denser 2 × 3 × 1 grid and a vacuum space of more than 15 Å was used to prevent the interaction between the two periodic cells. The setting of the BiOBr (001) model is similar. The force tolerance, total energy, maximum stress, and maximum displacement at relaxation converge to 0.05 eV/Å, 2.0 × 10^{-5} eV/atom, 0.1 GPa, and 0.002 Å, respectively. The DFT−D dispersion correction scheme of TS is used to describe the van der Waals (vdW) interactions in these systems. The calculation of work function adopts the formula $\Phi = E_V - E_F$, where E_V represents the electrostatic potential of vacuum and E_F represents the electrostatic potential of Fermi level.

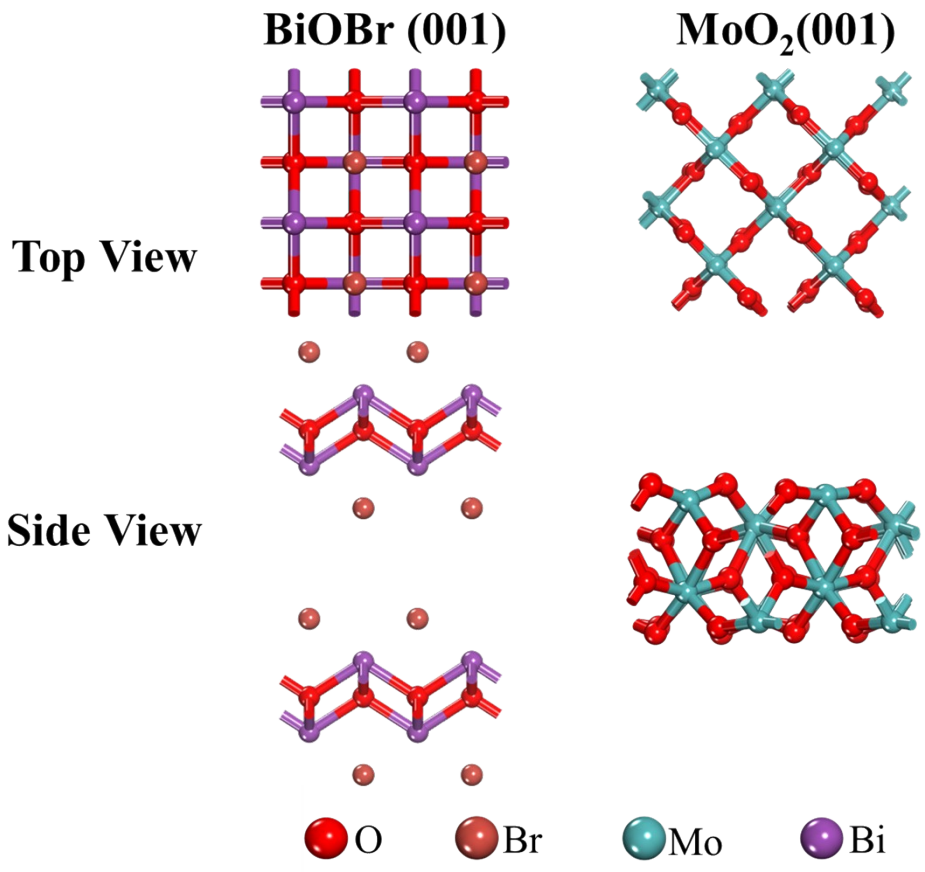

Figure S3. Optimized structure of top and side views of BiOBr(001) and MoO2(001) surfaces

4. Photo-deposition experiment of Ag on BiOBr

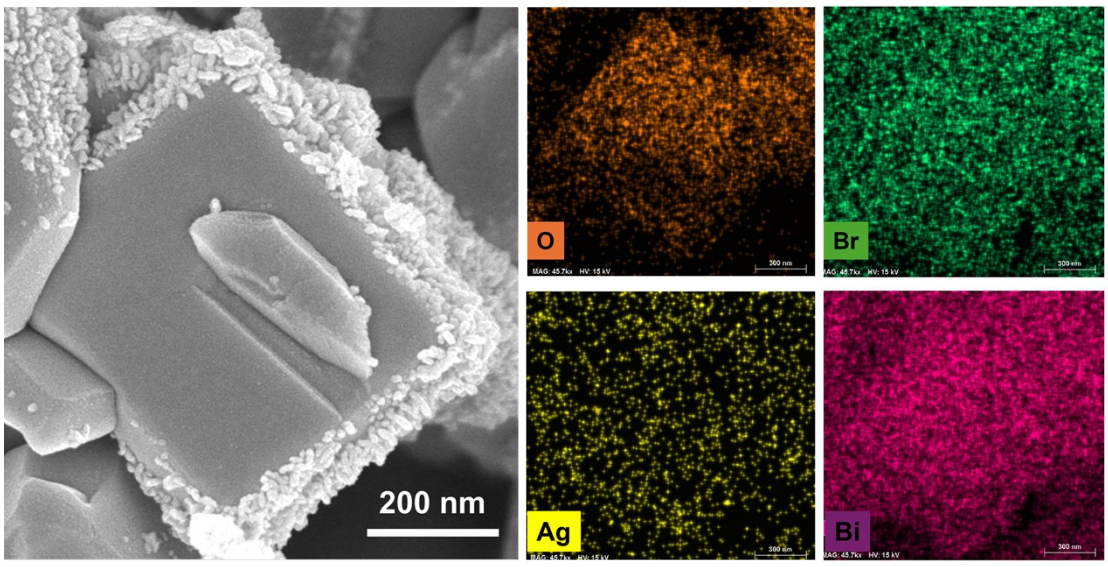

Figure S4. Photo-deposition experiment results of Ag on BiOBr nanosheet

5. The variation of ammonia generation rate over time for different materials

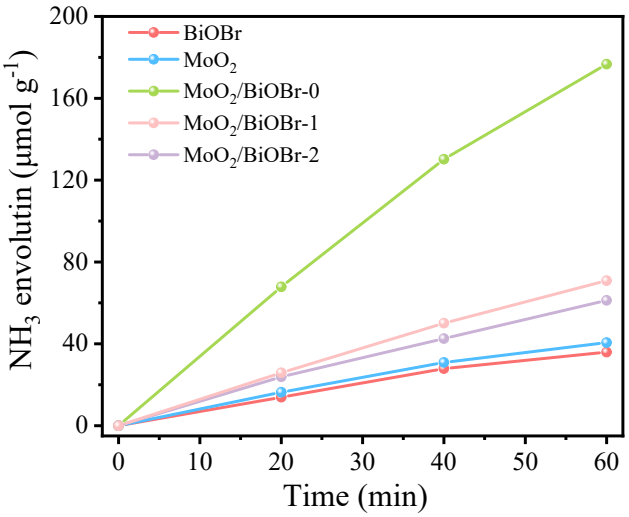

Figure S5. The variation of ammonia generation rate over time for different materials

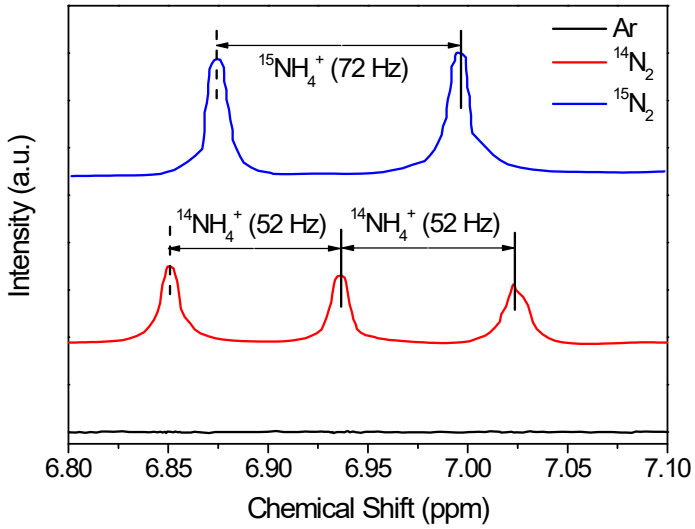

Figure S6. The results of $^{15}N_2$ isotope labeling by NMR spectrum for MoO_2/BiOBr-0.

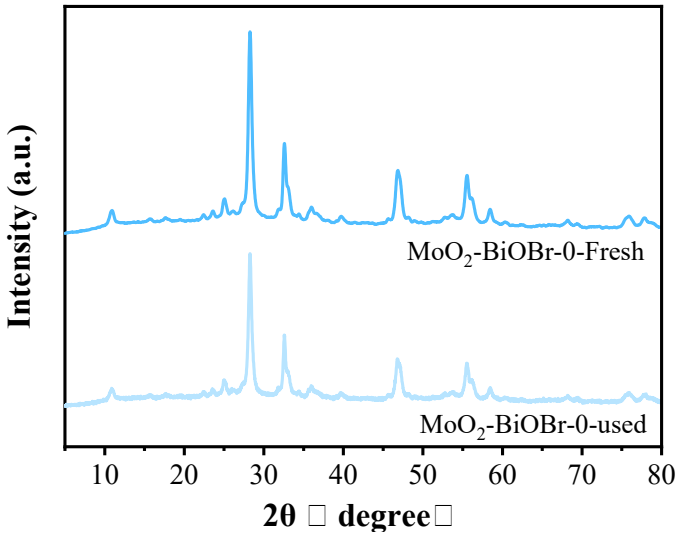

Figure S7. the XRD characterization results of MoO_2/BiOBr-0 before and after reaction.

6. The measurement of the average decay lifetime (τ_{av})

The typical TRPL decay curves for all samples are fitted by exponential decay kinetics function expressed as follows Eq. (S1):

$$I(t) = \sum_{i=1,2} B_i \cdot \exp(t / \tau_i) \quad \text{(S1)}$$

Here, the τ_{av} is determined by Eq. (S2) below:

$$\tau_{av} = \sum_{i=1,2} B_i \cdot \tau_i^2 / \sum_{i=1,2} B_i \cdot \tau_i \quad \text{(S2)}$$

where τ_1, τ_2 are the decay times for the faster and the slower components, B_1, B_2 are the contribution of each component, τ_{av} is the average decay time. The detailed information is listed in **Table S1**.

Table S1. Summarizing the information about the lifetime components (τ_i), contribution of each component (B_i) and average lifetime (τ_{av}) for BiOBr, MoO_2, MoO_2/BiOBr-2, MoO_2/BiOBr-1, and MoO_2/BiOBr-0.

Sample	τ_1 (ns)	τ_2 (ns)	B_1	B_2	τ_{av} (ns)
BiOBr	0.604	7.576	0.942	0.017	1.76
MoO_2	0.417	12.985	1.471	0.012	2.87

MoO_2/BiOBr-2	0.375	14.869	1.523	0.010	4.99
MoO_2/BiOBr-1	0.321	17.103	1.645	0.009	5.75
MoO_2/BiOBr-0	0.204	23.452	1.824	0.006	9.14

7. Measurement of BIEF variation

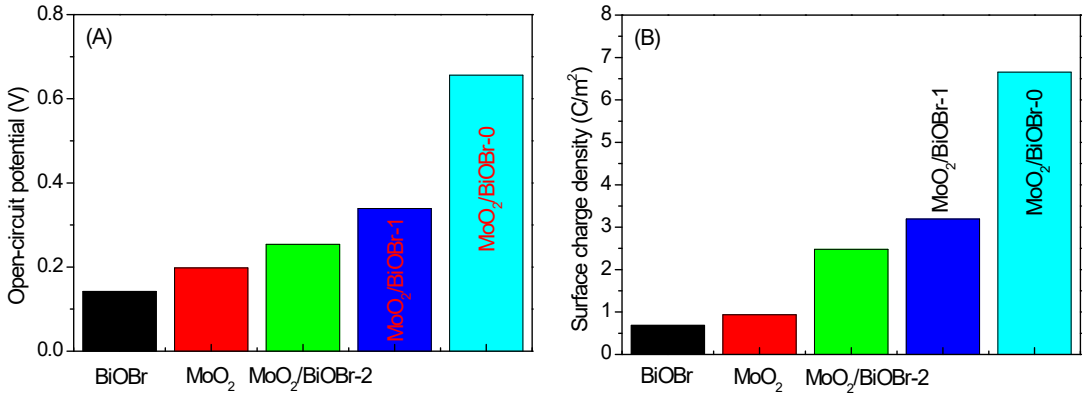

Figure S8. Open-circuit potentials (A) and surface charge densities (B) of all samples.

We calculated the variation of BIEF magnitude of the BiOBr, MoO_2 and MoO_2/BiOBr catalysts by using the model (Eq. (S3)) developed by Kanata *et al* [1-3].

$$F_S = (-2V_S\rho / \varepsilon\varepsilon_0)^{1/2} \quad \text{(S3)}$$

Where F_s is the BIEF magnitude, V_s is the surface voltage, ρ is the surface charge density, $\mathcal{E}$ is the low-frequency dielectric constant, and $\mathcal{E}_0$ is the permittivity of free space. Eq. S3 reveals that the BIEF magnitude is mainly determined by the surface voltage and the charge density because $\mathcal{E}$ and $\mathcal{E}_0$ are two constants. In order to evaluate the BIEF magnitude variation in samples, we carefully figured out their surface voltages by open-circuit potentials measurements and charge densities by the simultaneous potentiometric and conductimetric titrations method, which were shown in **Figure S8** [4-6].

Surface charge density of samples was calculated by applying Eq. (S4) and using *K1* and *K2* values obtained from the simultaneous potentiometric and conductimetric titrations. The equilibrium constants *K1* and *K2* can be experimentally determined by the application of Henderson–Hasselbach equation in the simultaneous potentiometric and conductimetric titration data. From equilibrium constants, the surface charge

density of samples s as function of pH values can be calculated by the following Eq. (S4).

$$\rho_0 = (\frac{F}{A})[(\frac{10^{-2pH} - K_1K_2}{10^{-2pH} + 10^{-2pH}K_1 + K_1K_2})N_T] \quad \text{(S4)}$$

Where F is the Faraday constant, A is the total surface area, NT is the total number of moles of surface sites, and *K1* and *K2* are the acid equilibrium constants, pH is the value for preparing the sample.

8. Measurement of bulk-charge separation efficiency (η_{bulk})

The photoelectrodes were prepared according to our previously reported method [7,8]. The indium doped tin oxide (ITO, China Southern Glass Co., Ltd., Shenzhen, China) substrates were first ultrasonically cleaned in distilled water, absolute ethanol, and isopropanol for 15 min sequentially. Both edges of the conducting glass substrates were then covered with adhesive tape. Typically, the aqueous slurries of the samples were spread on an ITO glass substrate with a glass rod, using adhesive tapes as spaces. The suspension was prepared by grinding 20 mg of samples, 40 μL of PEDOT-PSS (Sigma-Aldrich, 1.3-1.7%) aqueous solution, and 200 μL of water. The resulting film was dried in air and annealed at 150 °C for 10 min, yielding an electrode with catalyst loading amount of ca. 0.254 mg cm^{-2}. The photocurrents were measured by an electrochemical analyzer (CHI660D, Shanghai, China) in a standard three-electrode system with the samples as the working electrodes, a Pt foil as the counter electrode, and a saturated calomel electrode (SCE) as a reference electrode. A 150 W Xe arc lamp equipped with a 420 nm cutoff filter ($\lambda \geq 420$ nm) was utilized as a light source.

We measured the η_{bulk} in the BiOBr, MoO_2 and MoO_2/BiOBr catalysts and other reference samples by the method recently reported by Choi's group and Gong's group [9,10]. Briefly, the measured photocurrent densities (J) obey the following Eq. (S5):

$$J = J_{abs} \times \eta_{bulk} \times \eta_{surface} \quad \text{(S5)}$$

where J_{abs} is the current density converted from the absorbed photons when assuming that the absorbed photons were completely converted into electrons, η_{bulk} is the

efficiency of e-h separation in the bulk of photocatalyst, and $\eta_{surface}$ is the efficiency of e-h separation on the surface of photocatalyst. When adding 1 M Na_2SO_3 as hole scavenger to the above system of photocurrent measurement, we assume that Na_2SO_3 can completely hinder the e-h recombination on the surface of photocatalyst without affecting e-h separation in the bulk of photocatalyst. In this case $\eta_{surface}$ is assumed to be 1, so η_{bulk} can be determined as follows:

$$\eta_{bulk} = J_{sulfite} / J_{abs} \quad \text{(S6)}$$

where *J*sulfite is the photocurrent density in the presence of Na_2SO_3.

The photocurrent densities were measured by using Na_2SO_3 as electrolytes. The purple curves in **Figure S9** are the current density distribution converted from the light intensity of a 150 W Xe arc lamp equipped with a 420 nm cutoff filter ($\lambda \geq 420$ nm). This conversion was based on the equation: (1) $J_{abs} = (Nq)/t$, where t, N, and q were the irradiation time, the number of incident photons during the irradiation time t, and the charge of a single electron, and (2) $N = (E_\lambda)/(hc)$, where E, λ, h, and c are the energy of incident photons, the wavelength of the incident monochromatic light, the Planck constant, and the light speed, respectively.

The J_{abs} shown in **Figure S10** is calculated by using Eq. (7):

$$J_{abs} = \int_a^b f(x)d(x) \quad (7)$$

where a is the shortest wavelength of the light emitted by the 150 W Xe arc lamp equipped with a 420 nm cutoff filter ($\lambda \geq 420$ nm), b is the wavelength of the photo-absorption edge of photocatalysts, and *f(x)* is the relationship formula between the light-converted current density and irradiation wavelength (x) of the 150 W Xe arc lamp equipped with a 420 nm cutoff filter ($\lambda \geq 420$ nm).

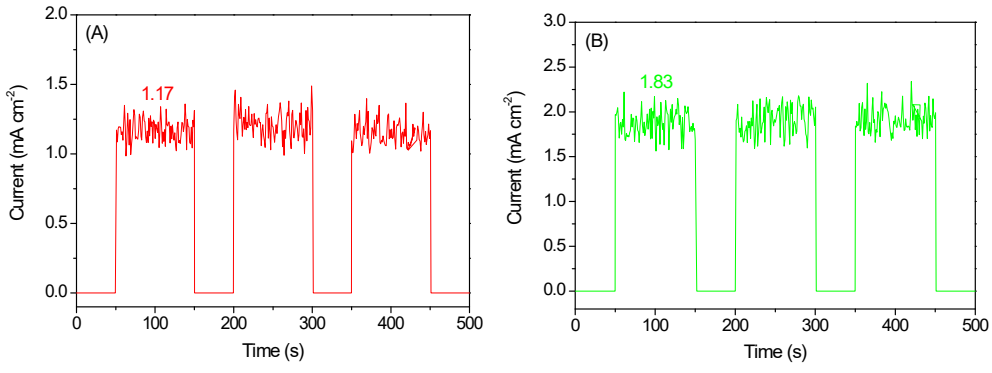

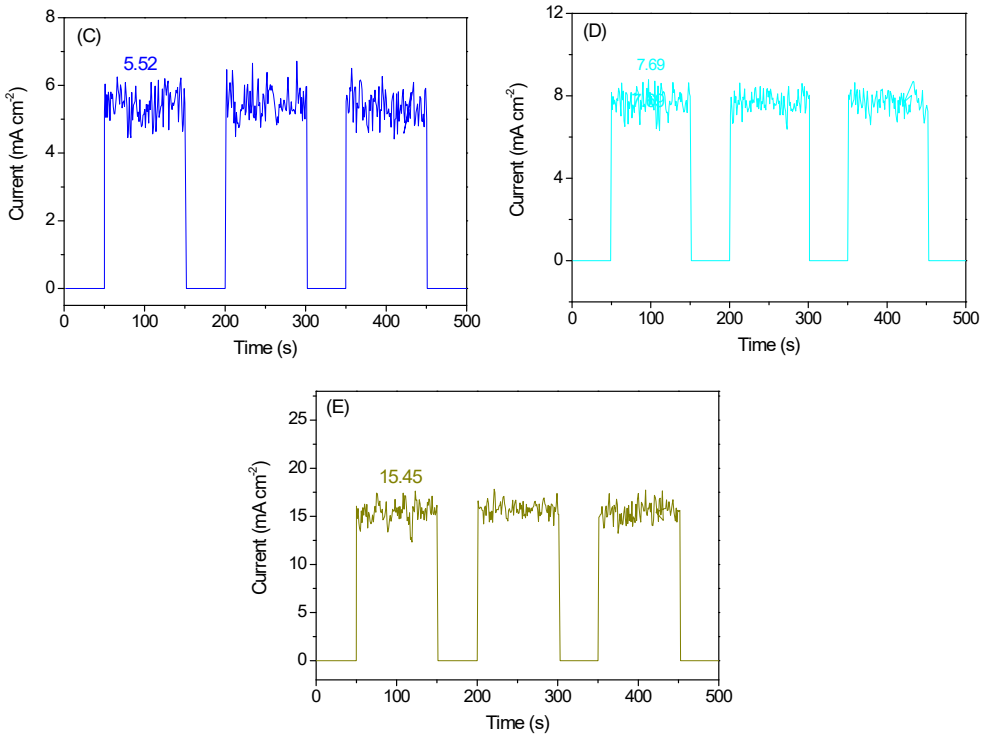

Figure S9. Transient photocurrent responses of five samples: A is BiOBr, B is MoO_2, C is MoO_2/BiOBr-2, D is MoO_2/BiOBr-1, E is MoO_2/BiOBr-0.

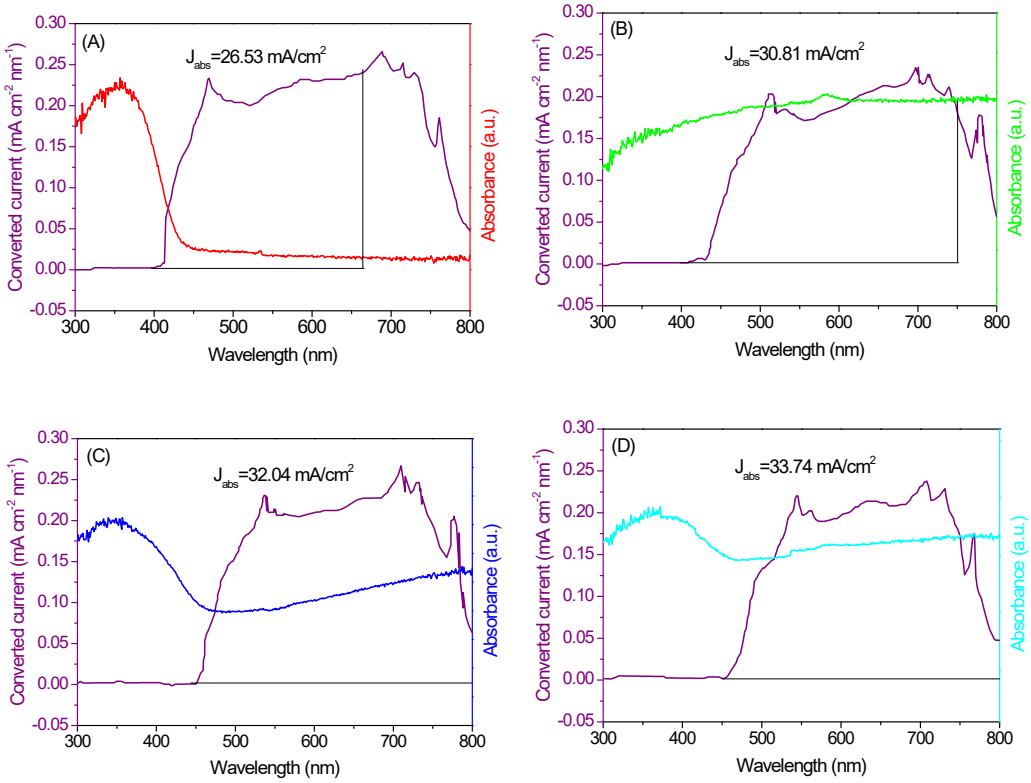

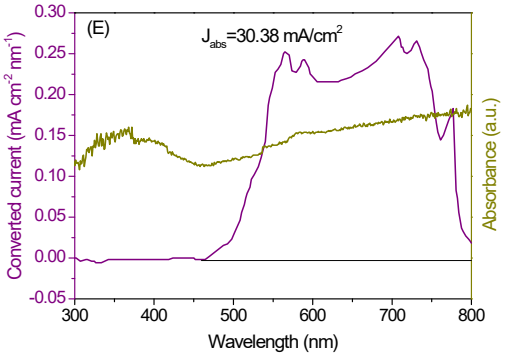

Figure S10. UV–visible diffuse reflectance spectrum and the value of J_{abs} of five samples: A is BiOBr, B is MoO_2, C is MoO_2/BiOBr-2, D is MoO_2/BiOBr-1, E is MoO_2/BiOBr-0.

Reference

[1] Lefebvre, P.; Allegre, J.; Gil, B.; Mathieu, H. *Phys. Rev. B* **1999**, *59*, 15363;

[2] Morello, G.; Sala, F. D.; Carbone, L.; Manna, L.; Maruccio, G.; Cingolani, R.; Giorgi, M. D. *Phys. Rev. B* **2008**, *78*, 195313;

[3] Im, J. S.; Kollmer, H.; Off, Sohmer, J. A.; Scholz, F.; Hangleiter, A. *Phys. Rev. B* **1998**, *57*, R9435;

[4] Yanina, S. V.; Rosso, K. M.; *Science* **2008**, *320*, 218;

[5] Prado, A. G. S.; Bolzon, L. B.; Pedroso, C. P.; Moura, A. O.; Costa, L. L. *Appl. Catal. B* **2008**, *82*, 219;

[6] Kallay, N.; Madic, T.; Kucej, K.; Preocanin, T. *Colloids Surf. A* **2003**, *230*, 3.

[7] Li, R.; Hu, J. H.; Deng, M. S.; Wang, H. L.; Wang, X. J.; Hu, Y. L.; Jiang, H. L.; Jiang, J.; Zhang, Q.; Xie, Y.; Xiong, Y. J. *Adv. Mater.* **2014**, *26*, 4783;

[8] Lei, F. C.; Zhang, L.; Sun, Y. F.; Liang, L.; Liu, K. T.; Xu, J. Q.; Zhang, Q.; Pan, B. C.; Luo, Y.; Xie, Y. *Angew. Chem. Int. Ed.* **2015**, *54*, 9266;

[9] Kim, T. W.; Choi, K. S. *Science* **2014**, *343*, 990;

[10] Chang, X. X.; Wang, T.; Zhang, P.; Zhang, J. J.; Li, A.; Gong, J. L. *J. Am. Chem. Soc.* **2015**, *137*, 8356.